

# [Weak] Gravitational Lensing

Martin Kilbinger

CEA Saclay, Irfu/SAp - AIM; IAP

Euclid Summer School, Narbonne  
August 22 – 27, 2016

`martin.kilbinger@cea.fr`

`www.cosmostat.org/kilbinger`

Slides: <http://www.cosmostat.org/ecole16>



`@energie_sombre`

# Overview

## Day 1: Principles of gravitational lensing

- Brief history of gravitational lensing
- Light deflection in an inhomogeneous Universe
- Convergence, shear, and ellipticity
- Projected power spectrum
- Real-space shear correlations

## Day 2: Measurement of weak lensing

- Galaxy shape measurement
- PSF correction
- Photometric redshifts
- Estimating shear statistics

## Day 3: Surveys and cosmology

- Cosmological modelling
- Results from past and ongoing surveys (CFHTLenS, KiDS, DES)
- Euclid

## Day 3+: Extra stuff

# Books, Reviews and Lecture Notes

- Bartelmann & Schneider 2001, review **Weak gravitational lensing**, Phys. Rep., 340, 297 arXiv:9912508
- Kochanek, Schneider & Wambsganss 2004, book (Saas Fee) **Gravitational lensing: Strong, weak & micro**, The third part (weak lensing) is available here: <http://www.astro.uni-bonn.de/~peter/SaaSFee.html>
- Kilbinger 2015, review **Cosmology from cosmic shear observations** Reports on Progress in Physics, 78, 086901, arXiv:1411.0155
- Henk Hoekstra 2013, lecture notes (Varenna) arXiv:1312.5981
- Sarah Bridle 2014, lecture videos (Saas Fee) <http://saasfee2014.epfl.ch/page-110036-en.html>
- Alan Heavens, 2015, lecture notes (Rio de Janeiro) [www.on.br/cce/2015/br/arq/Heavens\\_Lecture\\_4.pdf](http://www.on.br/cce/2015/br/arq/Heavens_Lecture_4.pdf)

# Science with gravitational lensing

## Outstanding results

Dark matter is not in form of massive compact objects (MACHOs).

Detection of Earth-mass exoplanets.

Structure of QSO inner emission regions.

Dark matter profiles in outskirts of galaxies.

Galaxy clusters are dominated by dark matter.

Constraints on dark energy and modified gravity.

## Most important properties of gravitational lensing

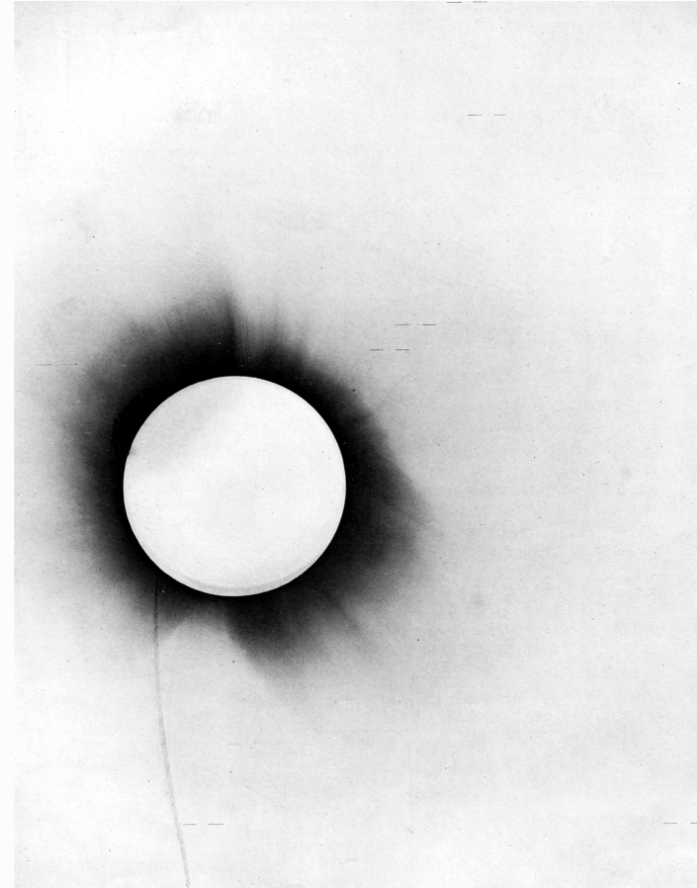
Lensing probes **total** matter, baryonic + dark.

Independent of dynamical state of matter.

Independent of nature of matter.

# Brief history of gravitational lensing

- Before Einstein: Masses deflect photons, treated as point masses.
- 1915 Einstein's GR predicted deflection of stars by sun, deflection larger by 2 compared to classical value. Confirmed 1919 by Eddington and others during solar eclipse.



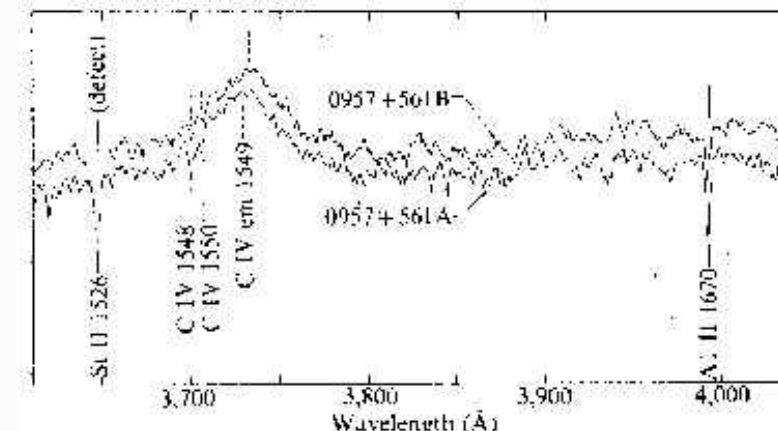
Photograph taken by Eddington of solar corona, and stars marked with bars.

# Lensing on cosmological scales



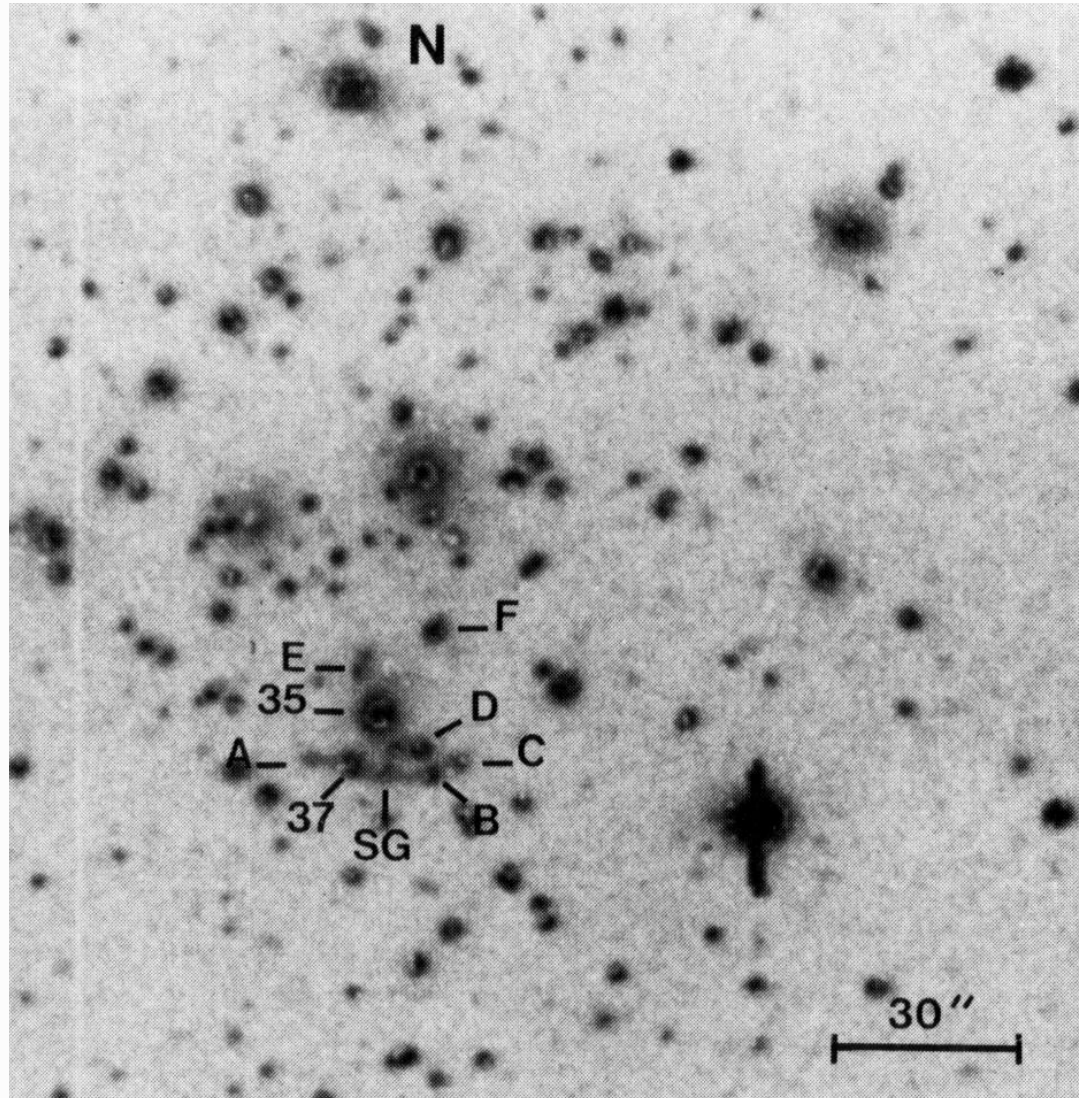
Fritz Zwicky; Abell 2151 (Hercules galaxy cluster) ©Tony Hallas/APoD.

- 1937 Zwicky posits galaxy clusters as lenses.
- 1979 Walsh et al. detect first double image of a lenses quasar.



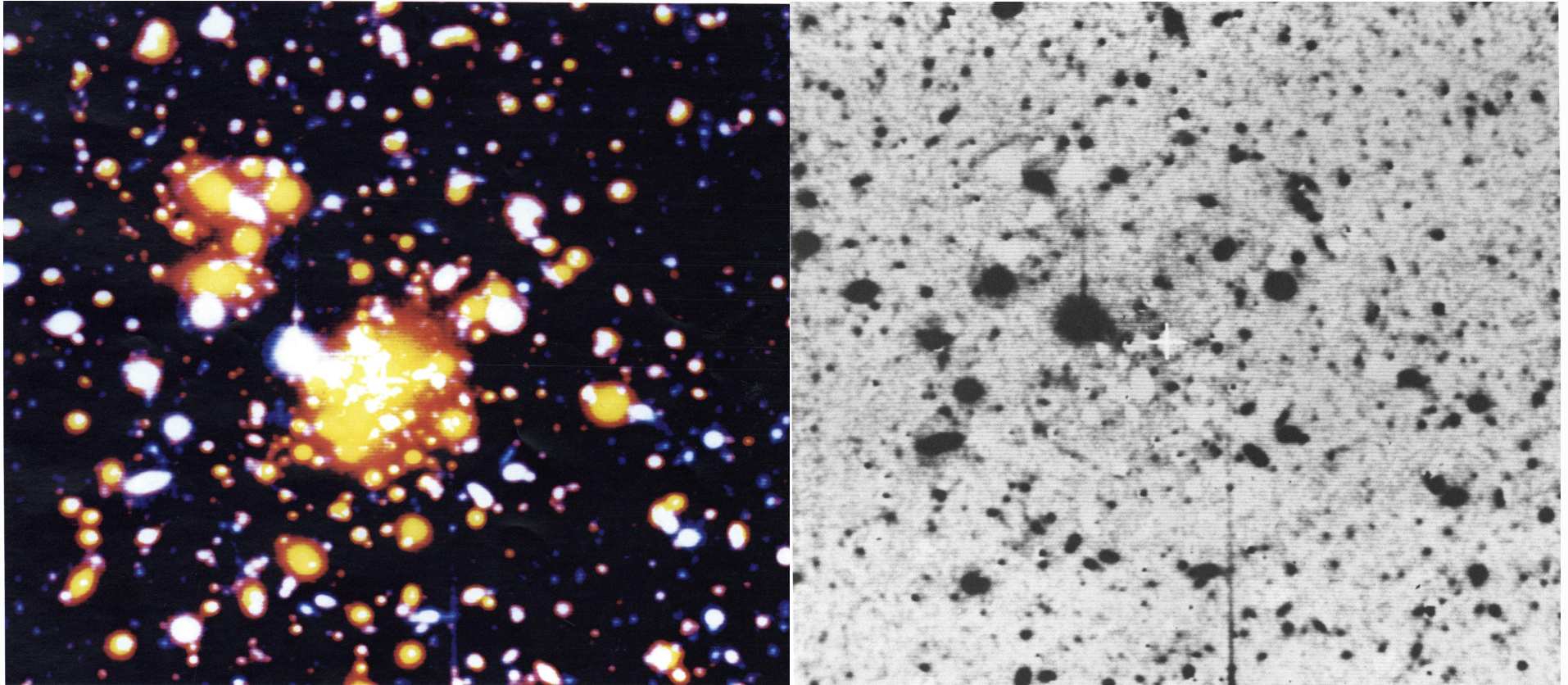
(Walsh et al. 1979)

- 1987 Soucail et al. strongly distorted “arcs” of background galaxies behind galaxy cluster, using CCDs.



exclude that it is an off-chance superimposition of faint cluster galaxies even if a diffuse component seems quite clear from the R CCD field. A gravitational lens effect on a background quasar is a possibility owing to the curvature of the structure but in fact it is too small (Hammer 86) and no blue object opposite the central galaxy has been detected. It is more likely that we are dealing with a star formation region located in the very rich core where

- Tyson et al. (1990), tangential alignment around clusters.



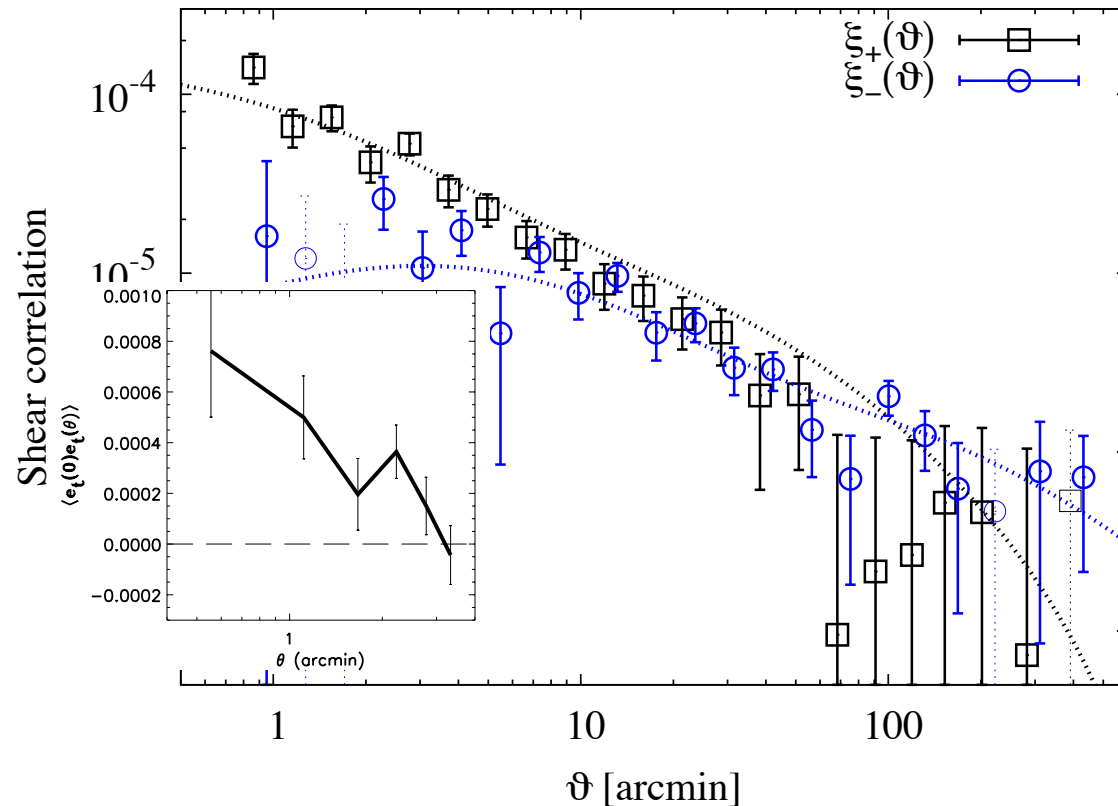
Abell 1689

Cluster outskirts: Weak gravitational lensing.



- 2000 **cosmic shear**: weak lensing in blind fields, by 4 groups (Edinburgh, Hawai'i, Paris, Bell Labs/US).

Some 10,000 galaxies on few square degree on the sky area.

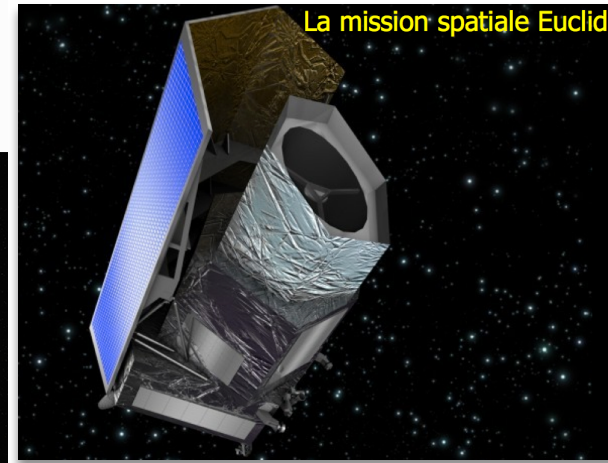
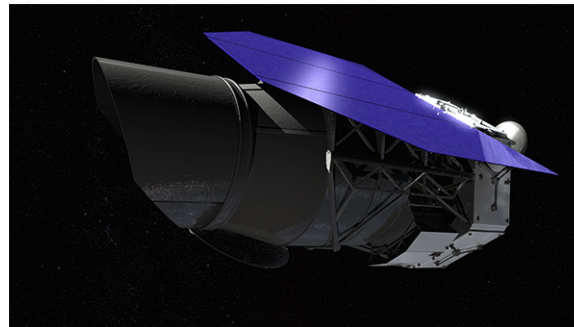
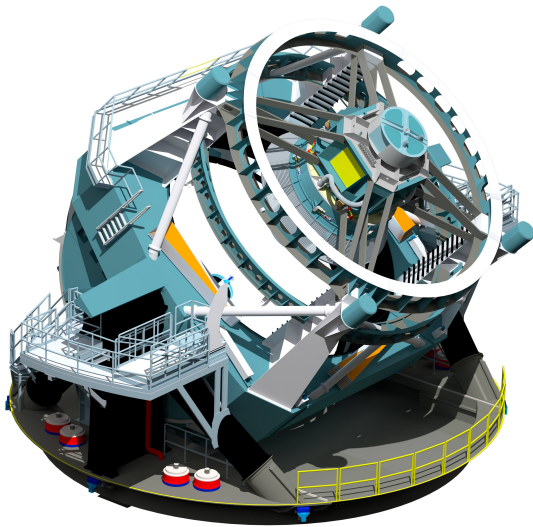
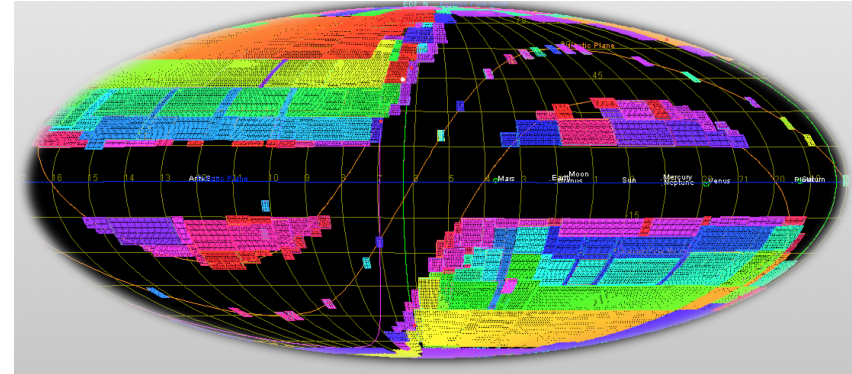


Shear (ellipticity)  
correlation of galaxies as  
fct. of angular separation  
(Van Waerbeke  
et al. 2000, Kilbinger  
et al. 2013).

- By 2016: Many dedicated surveys: DLS, CFHTLenS, DES, KiDS, HSC. Competitive constraints on cosmology.

Factor 100 increase: Millions of galaxies over 100s of degree area. Many other improvements: Multi-band observations, photometric redshifts, image and  $N$ -body simulations, ....

- By 2025: LSST, WFIRST-AFTA, Euclid data will be available.  
Another factor of 100 increase:  
Hundred millions of galaxies, tens of thousands of degree area (most of the extragalactic sky).



# Types of lensing

source	lens	observation	name	science
star	star ( $\neq$ sun)	time-varying magnification	micro-lensing	exoplanets, MACHOs, limb darkening
galaxy	galaxy, cluster	multiple images, arcs, $\Delta t$	strong lensing	galaxy $M/L$ , properties inner cluster structure, dark-matter properties, $H_0$ , QSO structure
galaxies	galaxies, cluster LSS	distortions, magnification, $\sigma$ (number density)	weak lensing	galaxy $M/L$ , halos, cluster $M$ , outer structure, cosmo parameters
CMB	LSS	distortions in $T$	CMB (weak) lensing	cosmo parameters

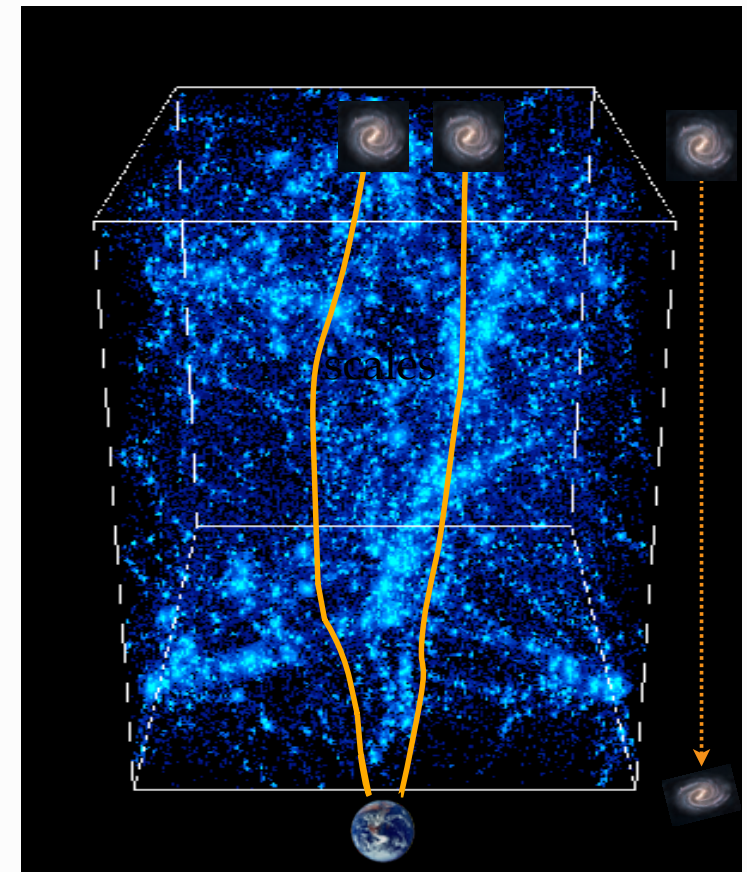
# Types of lensing

source	lens	observation	name	science
star	star ( $\neq$ sun)	time-varying magnification	micro-lensing	exoplanets, MACHOs, limb darkening
galaxy	galaxy, cluster	multiple images, arcs, $\Delta t$	strong lensing	galaxy $M/L$ , properties inner cluster structure, dark-matter properties, $H_0$ , QSO structure
<b>galaxies</b>	galaxies, cluster <b>LSS</b>	<b>distortions</b> , magnification, $\sigma$ (number density)	<b>weak lensing</b>	galaxy $M/L$ , halos, cluster $M$ , outer structure, <b>cosmo parameters</b>
CMB	LSS	distortions in $T$	CMB (weak) lensing	cosmo parameters

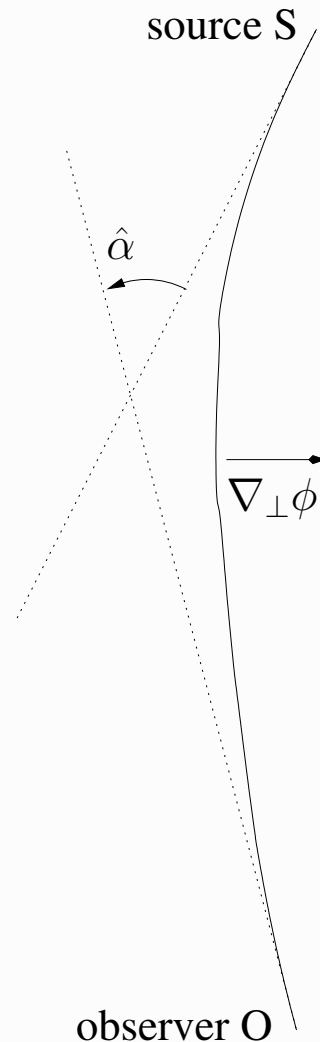
# Cosmic shear, or weak cosmological lensing

Light of distant galaxies is deflected while travelling through inhomogeneous Universe. Information about mass distributions is imprinted on observed galaxy images.

- Continuous deflection: sensitive to projected 2D mass distribution.
- Differential deflection: magnification, distortions of images.
- Small distortions, few percent change of images: need statistical measurement.
- Coherent distortions: measure correlations, scales few Mpc ... few 100 Mpc.



# Deflection angle



Perturbed Minkowski metric, weak-field ( $\phi \ll c^2$ )

$$ds^2 = (1 + 2\phi/c^2) c^2 dt^2 - (1 - 2\phi/c^2) dl^2$$

One way to derive deflection angle: Fermat's principle:

Light travel time  $t = \frac{1}{c} \int_{\text{path}} (1 - 2\phi/c^2) dl$

is stationary,  $\delta t = 0$ . (Analogous to geometrical optics, potential as medium with refract. index  $n = 1 - 2\phi/c^2$ .)  
Integrate Euler-Lagrange equations along the light path to get

deflection angle  $\hat{\alpha} = -\frac{2}{c^2} \int_S^O \nabla_{\perp} \phi dl$

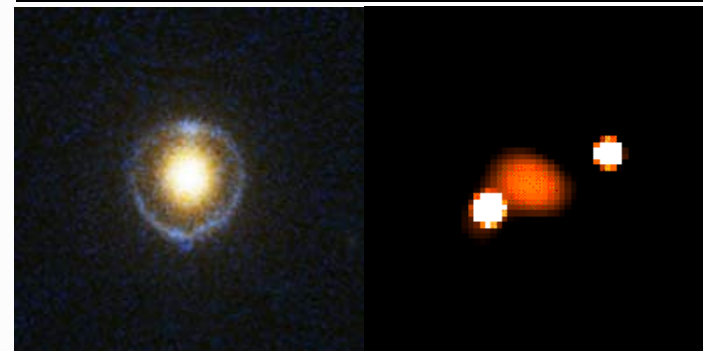
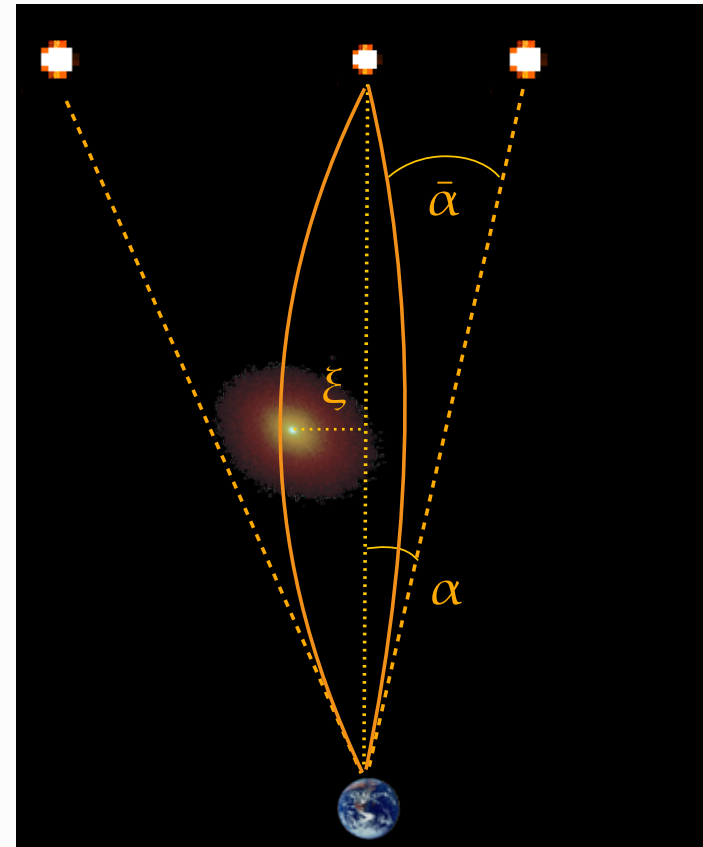
## Special case: point mass

Deflection angle for a point mass  $M$  is

$$\hat{\alpha} = \frac{4GM}{c^2} \frac{\xi}{\xi} = \frac{2R_S}{\xi} \frac{\xi}{\xi}$$

( $R_S$  is the Schwarzschild radius.)

This is twice the value one would get in a classical, Newtonian calculation.



SDSS J1627-0053

HE 1104-1825

$z_s = 0.5, z_l = 0.2, \alpha = 2.8''$  (5 kpc)

$z_s = 2.3, z_l = 1.7, \alpha = 1.6''$  (14 kpc)

## Exercise: Derive the deflection angle for a point mass. I

In the weak-field approximation, we can write the potential as

$$\phi = -\frac{GM}{R} = -\frac{c^2 R_S}{2 R},$$

where  $G$  is Newton's constant,  $M$  the mass of the object,  $R$  the distance, and  $R_S$  the Schwarzschild radius. The distance  $R$  can be written as  $R^2 = x^2 + y^2 + z^2$ .

(Here  $z$  is not redshift, but radial (comoving) distance.)

We use the so-called Born approximation (from quantum mechanic scattering theory) to integrate along the unperturbed light ray, which is a straight line parallel to the  $z$ -axis with a constant  $x^2 + y^2 = \xi^2$ . The impact parameter  $\xi$  is the distance of the light ray to the point mass.

The deflection angle is then

$$\hat{\alpha} = -\frac{2}{c^2} \int_{-\infty}^{\infty} \nabla_{\perp} \phi dz.$$



## Exercise: Derive the deflection angle for a point mass. II

The perpendicular gradient of the potential is

$$\nabla_{\perp} \phi = \frac{c^2 R_S}{2|R|^3} \begin{pmatrix} x \\ y \end{pmatrix} = \frac{c^2 R_S}{2} \frac{\xi}{(\xi^2 + z^2)^{3/2}} \begin{pmatrix} \cos \varphi \\ \sin \varphi \end{pmatrix}.$$

The primitive for  $(\xi^2 + z^2)^{-3/2}$  is  $z\xi^{-2}(\xi^2 + z^2)^{-1/2}$ . We use the symmetry of the integrand to integrate between 0 and  $\infty$ , and get for the absolute value of the deflection angle

$$\hat{\alpha} = 2R_S \left[ \frac{z}{\xi(\xi^2 + z^2)^{1/2}} \right]_0^{\infty} = \frac{2R_S}{\xi} = \frac{4GM}{c^2 \xi}.$$

## Generalisation I: mass distribution

Distribution of point masses  $M_i(\boldsymbol{\xi}_i, z)$ : total deflection angle is linear vectorial sum over individual deflections

$$\hat{\alpha}(\boldsymbol{\xi}) = \sum_i \hat{\alpha}(\boldsymbol{\xi} - \boldsymbol{\xi}_i) = \frac{4G}{c^2} \sum_i M(\boldsymbol{\xi}_i, z) \frac{\boldsymbol{\xi} - \boldsymbol{\xi}_i}{|\boldsymbol{\xi} - \boldsymbol{\xi}_i|}$$

With transition to continuous density

$$M_i(\boldsymbol{\xi}_i, z) \rightarrow \int d^2\xi' \int dz' \rho(\boldsymbol{\xi}', z')$$

and introduction of the 2D

$$\text{surface mass density } \Sigma(\boldsymbol{\xi}') = \int dz' \rho(\boldsymbol{\xi}', z')$$

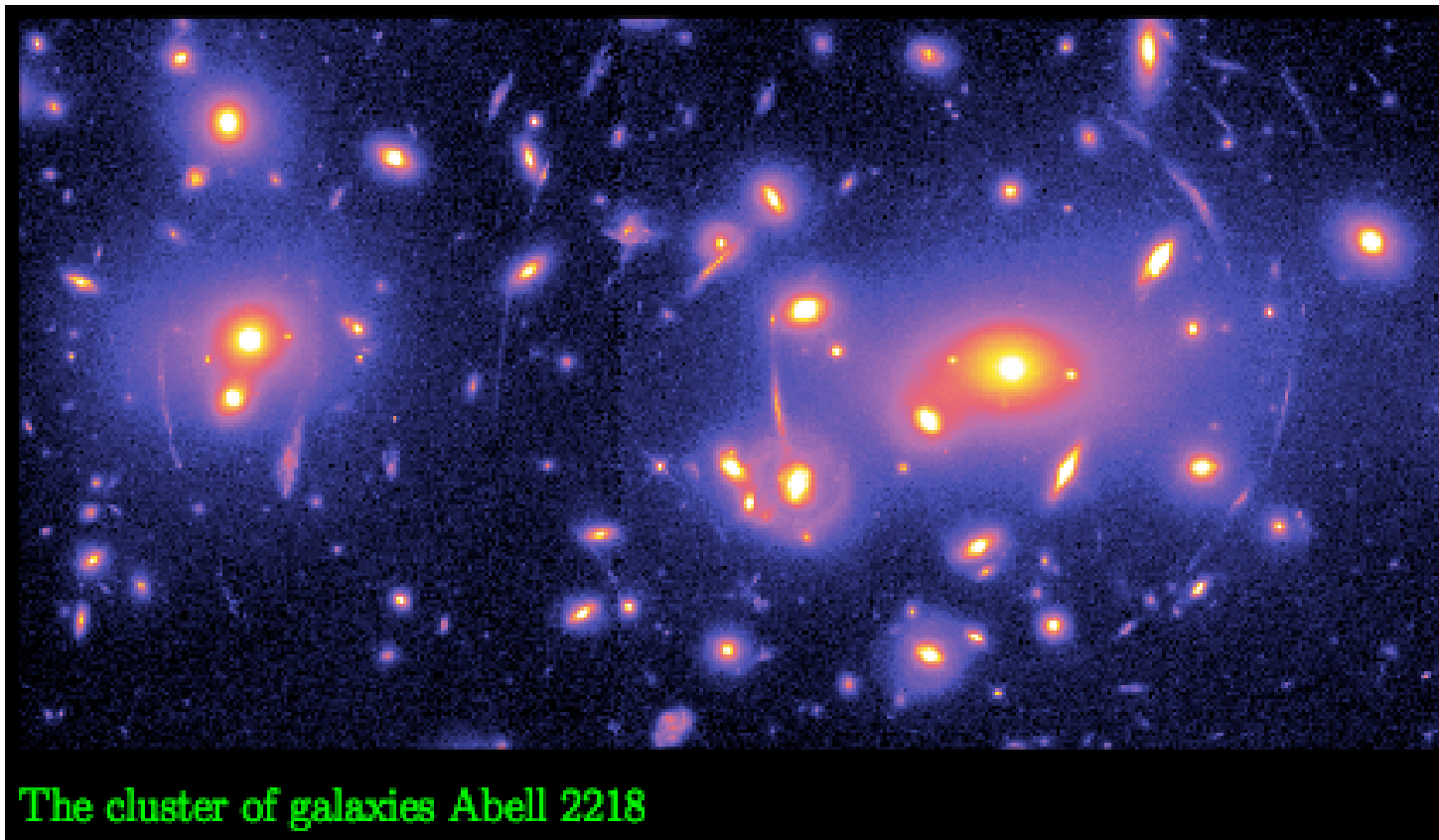
we get

$$\hat{\alpha}(\boldsymbol{\xi}) = \int d^2\xi' \Sigma(\boldsymbol{\xi}') \frac{\boldsymbol{\xi} - \boldsymbol{\xi}_i}{|\boldsymbol{\xi} - \boldsymbol{\xi}_i|}$$

**Thin-lens approximation**

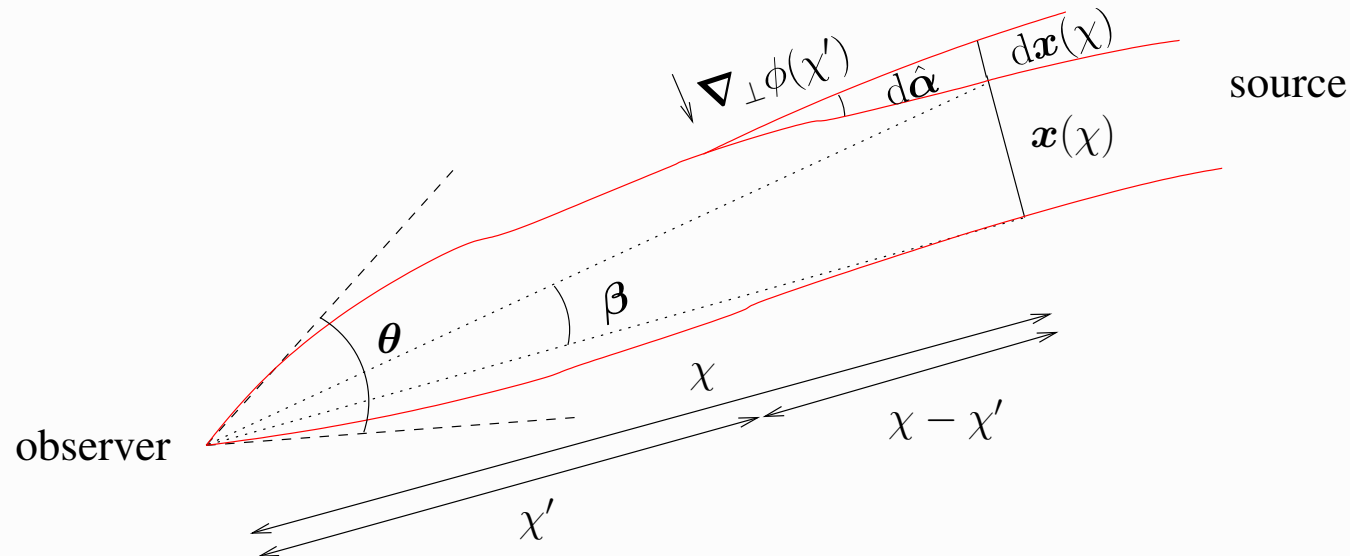
## Generalisation II: Extended source I

Extended source: different light rays impact lens at different positions  $\xi$ , their deflection angle  $\alpha(\xi)$  will be different: **differential deflection**  $\rightarrow$  distortion, magnification of source image!



# Propagation of light bundles I

Calculate deflection angle difference between different light bundles:



In homogeneous flat Universe, transverse distance  $\mathbf{x}_0$  between two light rays as fct. of comoving distance  $\chi$

$$\mathbf{x}_0(\chi) = \chi\boldsymbol{\theta}.$$

This is modified by inhomogeneous matter = deflectors as follows.

## Propagation of light bundles II

From deflector at comoving distance  $\chi'$ , infinitesimal deflection angle

$$d\hat{\alpha} = -\frac{2}{c^2} \nabla_{\perp} \phi(\mathbf{x}, \chi') d\chi'$$

This results in a change of transverse distance  $d\mathbf{x}$  from vantage point of deflector (at  $\chi'$ )

$$d\mathbf{x} = (\chi - \chi') d\hat{\alpha}$$

Total deflection: integrate over all deflectors along  $\chi'$ . This would yield the difference between a perturbed and an unperturbed light ray. To account for perturbation of second light ray, subtract gradient of potential  $\phi^{(0)}$  along second light ray.

$$\mathbf{x}(\chi) = \chi \boldsymbol{\theta} - \frac{2}{c^2} \int_0^{\chi} d\chi' (\chi - \chi') \left[ \nabla_{\perp} \phi(\mathbf{x}(\chi'), \chi') - \nabla_{\perp} \phi^{(0)}(\chi') \right].$$

Transform distances into angles seen from the observer: divide by  $\chi$ .  $\mathbf{x}/\chi$  is the angle  $\boldsymbol{\beta}$  under which the unlensed source is seen. The integral/ $\chi$  is the

## Propagation of light bundles III

geometric difference between unlensed ( $\beta$ ) and apparent, lensed ( $\theta$ ) is the **deflection angle**

$$\alpha = \frac{2}{c^2} \int_0^x d\chi' \frac{\chi - \chi'}{\chi} \left[ \nabla_{\perp} \Phi(\mathbf{x}(\chi'), \chi') - \nabla_{\perp} \Phi^{(0)}(\chi') \right].$$

This results in the **lens equation**

$$\beta = \theta - \alpha.$$

This is a mapping from lens coordinates  $\theta$  to source coordinates  $\beta$ . (Q: why not the other way round?)

## Linearized lensing quantities I

To 0<sup>th</sup> order: approximate light path  $\mathbf{x}$ , on which potential gradient is evaluated in integral with unperturbed line  $\chi\boldsymbol{\theta}$  (**Born approximation**):

$$\boldsymbol{\beta}(\boldsymbol{\theta}) = \boldsymbol{\theta} - \frac{2}{c^2} \int_0^{\chi} d\chi' \frac{\chi - \chi'}{\chi} \left[ \nabla_{\perp} \Phi(\chi'\boldsymbol{\theta}, \chi') - \nabla_{\perp} \Phi^{(0)}(\chi') \right].$$

This neglects coupling between structures at different distances (*lens-lens coupling*): Distortion at some distance adds to undistorted image, neglecting distortion effect on already distorted image by all matter up to that distance.

Numerical simulations show that Born is accurate to sub-percent on most scales. This is pretty cool. Differences between perturbed and unperturbed light ray can be a few Mpc!

Next, drop the second term (does not depend on distance  $\mathbf{x} = \chi\boldsymbol{\theta}$ , so gradient vanishes).

## Linearized lensing quantities II

Now, we can move the gradient out of integral. That means, deflection angle is a gradient of a potential, the 2D **lensing potential**  $\psi$ . Writing derivatives with respect to angle  $\boldsymbol{\theta}$ , we get

$$\boldsymbol{\beta}(\boldsymbol{\theta}, \chi) = \boldsymbol{\theta} - \nabla_{\boldsymbol{\theta}}\psi(\boldsymbol{\theta}, \chi)$$

with

$$\psi(\boldsymbol{\theta}, \chi) = \frac{2}{c^2} \int_0^\chi d\chi' \frac{\chi - \chi'}{\chi\chi'} \phi(\chi'\boldsymbol{\theta}, \chi').$$

[Note: Above equations are valid for flat Universe. For general (curved) models, some comoving distances are replaced by comoving angular distances.]



# Linearized lensing quantities III

## Linearizing lens equation

We talked about differential deflection before. To first order, this involves the derivative of the deflection angle.

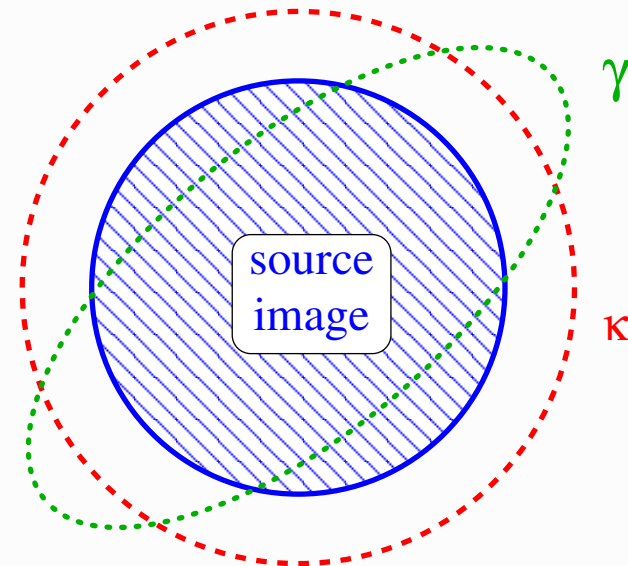
Or the lens mapping:

$$\frac{\partial \beta_i}{\partial \theta_j} \equiv A_{ij} = \delta_{ij} - \partial_i \partial_j \psi.$$

Jacobi (symmetric) matrix

$$A = \begin{pmatrix} 1 - \kappa - \gamma_1 & -\gamma_2 \\ -\gamma_2 & 1 - \kappa + \gamma_1 \end{pmatrix}.$$

- **convergence**  $\kappa$ : isotropic magnification
- **shear**  $\gamma$ : anisotropic stretching



Convergence and shear are second derivatives of the 2D lensing potential.

## Convergence and shear I

The effect of  $\kappa$  and  $\gamma$  follows from Liouville's theorem: Surface brightness is conserved (no photon gets lost).

Therefore the surface brightness  $I$  at the lensed position  $\boldsymbol{\theta}$  is equal to the unlensed, **source** surface brightness  $I^s$  at the source position  $\boldsymbol{\beta}$ .

$$I(\boldsymbol{\theta}) = I^s(\boldsymbol{\beta}(\boldsymbol{\theta})) \approx I^s(\boldsymbol{\beta}(\boldsymbol{\theta}_0) + \mathcal{A}(\boldsymbol{\theta} - \boldsymbol{\theta}_0))$$

### Example: circular isophotes

Effect can easily be seen for circular source isophotes, e.g.  $\theta_1 = R \cos t, \theta_2 = R \sin t$  (thus  $\theta_1^2 + \theta_2^2 = R^2$ ).

### Convergence

Applying the Jacobi matrix with zero shear (and setting  $\boldsymbol{\beta}(\boldsymbol{\theta}_0) = 0$ ), we find  $\beta_1^2 + \beta_2^2 = R^2(1 - \kappa)^2$ . The radius  $R$  of these isophotes gets transformed at source position to  $R(1 - \kappa)$ .

## Convergence and shear II

### Shear

To see an example for the shear stretching, set  $\gamma_2 = 0$ . We find

$(\beta_1, \beta_2) = R([1 - \kappa - \gamma_1] \cos t, [1 - \kappa + \gamma_1] \sin t)$  and thus

$(\beta_1/[1 - \kappa - \gamma_1])^2 + (\beta_2/[1 - \kappa + \gamma_1])^2 = R^2$ , which is an ellipse with half axes  $R/[1 - \kappa - \gamma_1]$  and  $R/[1 - \kappa + \gamma_1]$ .

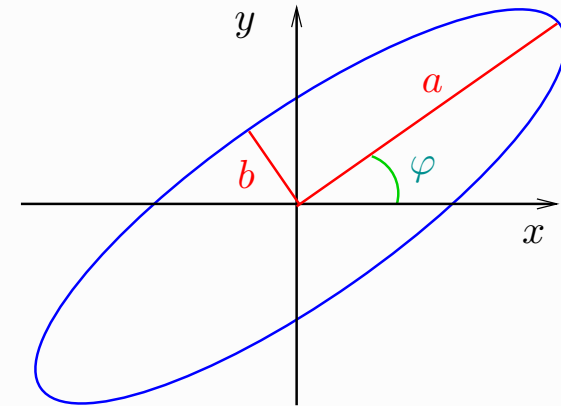
So we see that **shear** transforms a circular image into an elliptical one.

Define complex shear

$$\gamma = \gamma_1 + i\gamma_2 = |\gamma|e^{2i\varphi};$$

The relation between convergence, shear, and the axis ratio of elliptical isophotes is then

$$|\gamma| = |1 - \kappa| \frac{1 - b/a}{1 + b/a}$$



## Convergence and shear III

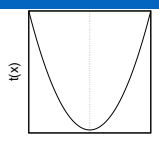
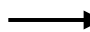
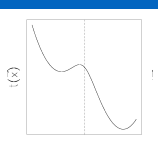

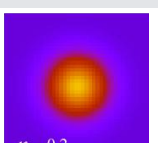
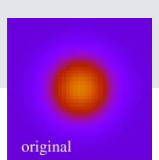
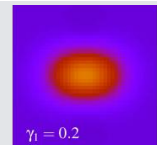
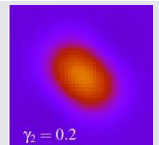
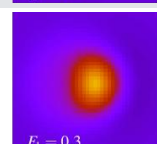
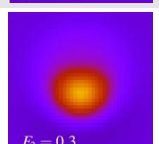
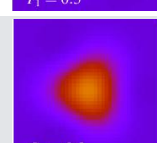
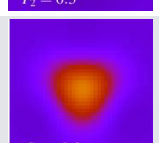
Further consequence of lensing: **magnification**.

Liouville (surface brightness is conserved) + area changes ( $d\beta^2 \neq d\theta^2$  in general)  $\rightarrow$  flux changes.

$$\text{magnification } \mu = \det A^{-1} = [(1 - \kappa)^2 - \gamma^2]^{-1}.$$

**Summary:** Convergence and shear linearly encompass information about projected mass distribution (lensing potential  $\psi$ ). They quantify how lensed images are magnified, enlarged, and stretched. These are the main observables in (weak) lensing.

# Effects of lensing, $\partial^i \psi / \partial x^i$

i	symbol	name	spin	effect
0	$\Delta t$	time delay	0	 $t(x)$ $x - x_c$   $t(x)$ $x - x_c$
1	$\alpha$	deflection	1	
2	$\kappa$	convergence	0	 $\kappa = 0.2$
2	$\gamma$	shear	2	  $\gamma_1 = 0.2$  $\gamma_2 = 0.2$
3	F	flexion	1	 $F_1 = 0.3$  $F_2 = 0.3$
3	G	flexion	3	 $G_1 = 0.3$  $G_2 = 0.3$

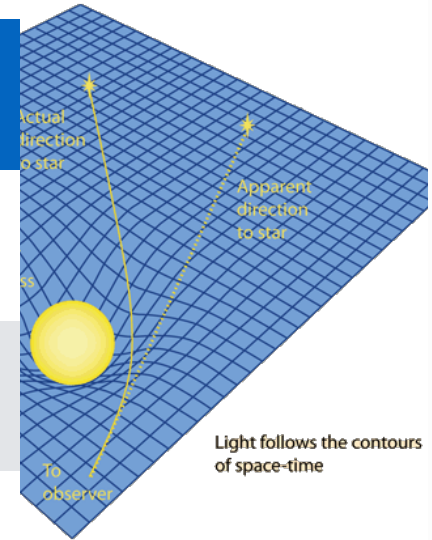


image credit Massimo

# Basic equation of weak lensing

## Weak lensing regime

$$\kappa \ll 1, |\gamma| \ll 1.$$

The observed ellipticity of a galaxy is the sum of the intrinsic ellipticity and the shear:

$$\varepsilon^{\text{obs}} \approx \varepsilon^{\text{s}} + \gamma$$

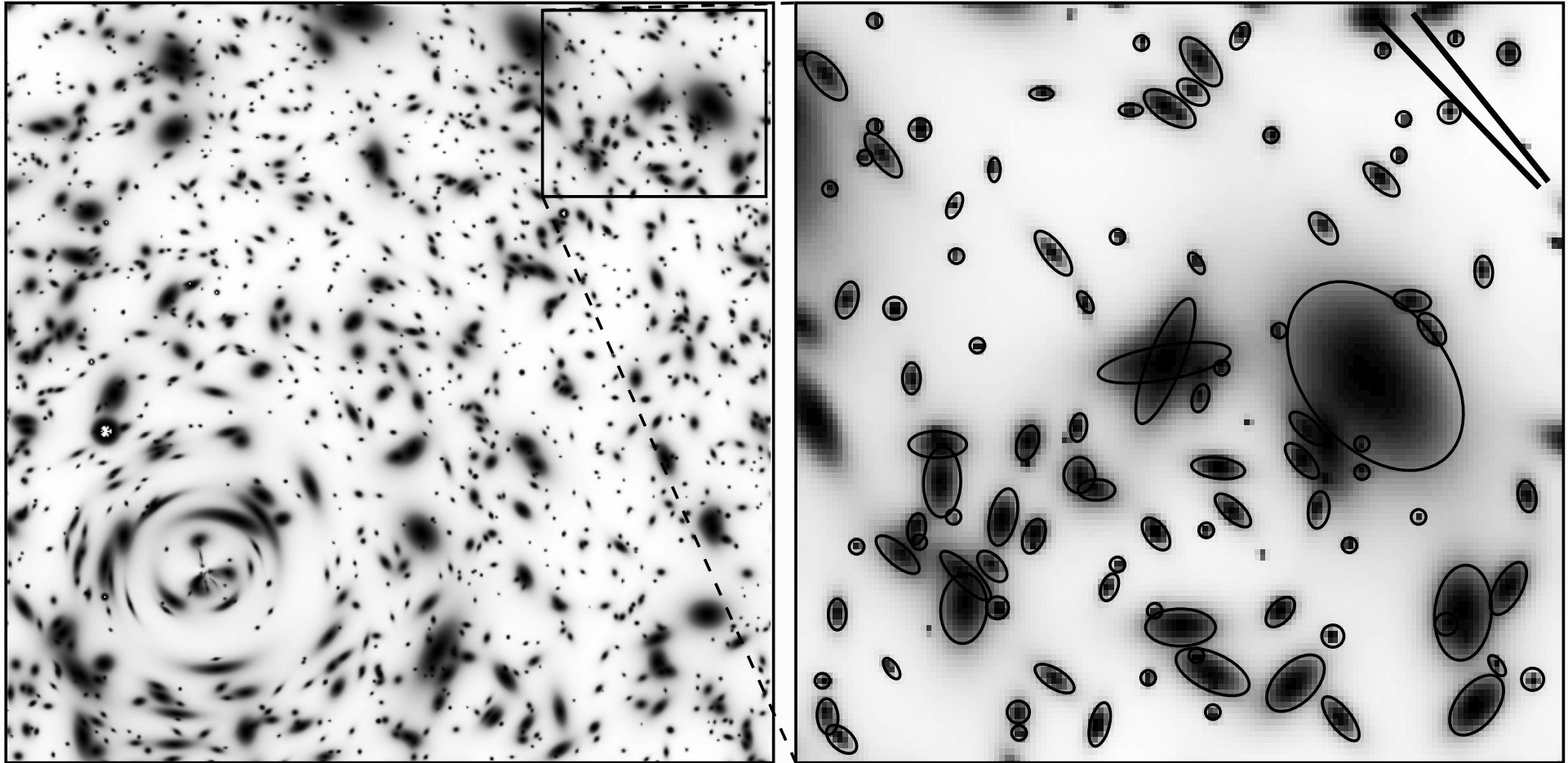
## Random intrinsic orientation of galaxies

$$\langle \varepsilon^{\text{s}} \rangle = 0 \quad \longrightarrow \quad \langle \varepsilon \rangle = \gamma$$

The observed ellipticity is an unbiased estimator of the shear. Very noisy though!  $\sigma_\varepsilon = \langle |\varepsilon^{\text{s}}|^2 \rangle^{1/2} \approx 0.4 \gg \gamma \sim 0.03$ . Increase  $S/N$  and beat down noise by averaging over large number of galaxies.

**Question:** Why is the equivalent estimation of the convergence and/or magnification more difficult?

## Ellipticity and local shear



[from Y. Mellier]

Galaxy ellipticities are an estimator of the local shear.

## Some weak-lensing galaxy surveys

Survey	Date	Area [deg <sup>2</sup> ]	$n_{\text{gal}}$ [arcmin <sup>-2</sup> ]
CFHTLenS	2003-2007	170	14
DLS	2001-2006	25	20
COSMOS	2005	1.6	80
SDSS	2000-2012	11,000	2
KiDS	2011-	1,500	7-8
HSC	2015-	1,500	~ 20
DES	2012-2018	5,000	5-6
LSST	2021-	15,000	~ 20
Euclid	2021-2026	15,000	~ 25
WFIRST-AFTA	2024-	2,500	?



# Convergence and cosmic density contrast

## Back to the lensing potential

- Since  $\kappa = \frac{1}{2}\Delta\psi$ :

$$\kappa(\boldsymbol{\theta}, \chi) = \frac{1}{c^2} \int_0^\chi d\chi' \frac{(\chi - \chi')\chi'}{\chi} \Delta\Phi(\chi'\boldsymbol{\theta}, \chi')$$

- Terms  $\Delta_{\chi'\chi'}\Phi$  average out when integrating along line of sight, can be added to yield 3D Laplacian (error  $\mathcal{O}(\Phi) \sim 10^{-5}$ ).
- Poisson equation

$$\Delta\Phi = \frac{3H_0^2\Omega_m}{2a} \delta \quad \left( \delta = \frac{\rho - \bar{\rho}}{\rho} \right)$$

$$\rightarrow \kappa(\boldsymbol{\theta}, \chi) = \frac{3}{2}\Omega_m \left( \frac{H_0}{c} \right)^2 \int_0^\chi d\chi' \frac{(\chi - \chi')\chi'}{\chi a(\chi')} \delta(\chi'\boldsymbol{\theta}, \chi').$$

# Amplitude of the cosmic shear signal

## Order-of magnitude estimate

$$\kappa(\boldsymbol{\theta}, \chi) = \frac{3}{2} \Omega_m \left( \frac{H_0}{c} \right)^2 \int_0^\chi d\chi' \frac{(\chi - \chi')\chi'}{\chi a(\chi')} \delta(\chi' \boldsymbol{\theta}, \chi').$$

for simple case: single lens at redshift  $z_L = 0.4$  with comoving size  $R/a(z_L)$ , source at  $z_S = 0.8$ .

$$\kappa \approx \frac{3}{2} \Omega_m \left( \frac{H_0}{c} \right)^2 \frac{D_{LS} D_L}{D_S} \frac{R}{a^2(z_L)} \frac{\delta\rho}{\rho}$$

Add signal from  $N \approx D_S/R$  crossings, calculate rms:

$$\begin{aligned} \langle \kappa^2 \rangle^{1/2} &\approx \frac{3}{2} \Omega_m \frac{D_{LS} D_L}{R_H^2} \sqrt{\frac{R}{D_S}} a^{-1.5}(z_L) \left\langle \left( \frac{\delta\rho}{\rho} \right)^2 \right\rangle^{1/2} \\ &\approx \frac{3}{2} 0.3 \times 0.1 \times 0.1 \times 2 \times 1 \approx 0.01 \end{aligned}$$

We are indeed in the weak-lensing regime.

## Convergence with source redshift distribution

So far, we looked at the convergence for one **single** source redshift (distance  $\chi$ ). Now, we calculate  $\kappa$  for a realistic survey with a redshift **distribution** of source galaxies. We integrate over the pdf  $p(\chi)d\chi = p(z)dz$ , to get

$$\kappa(\boldsymbol{\theta}) = \int_0^{\chi_{\text{lim}}} d\chi p(\chi) \kappa(\boldsymbol{\theta}, \chi) = \int_0^{\chi_{\text{lim}}} d\chi G(\chi) \chi \delta(\chi\boldsymbol{\theta}, \chi)$$

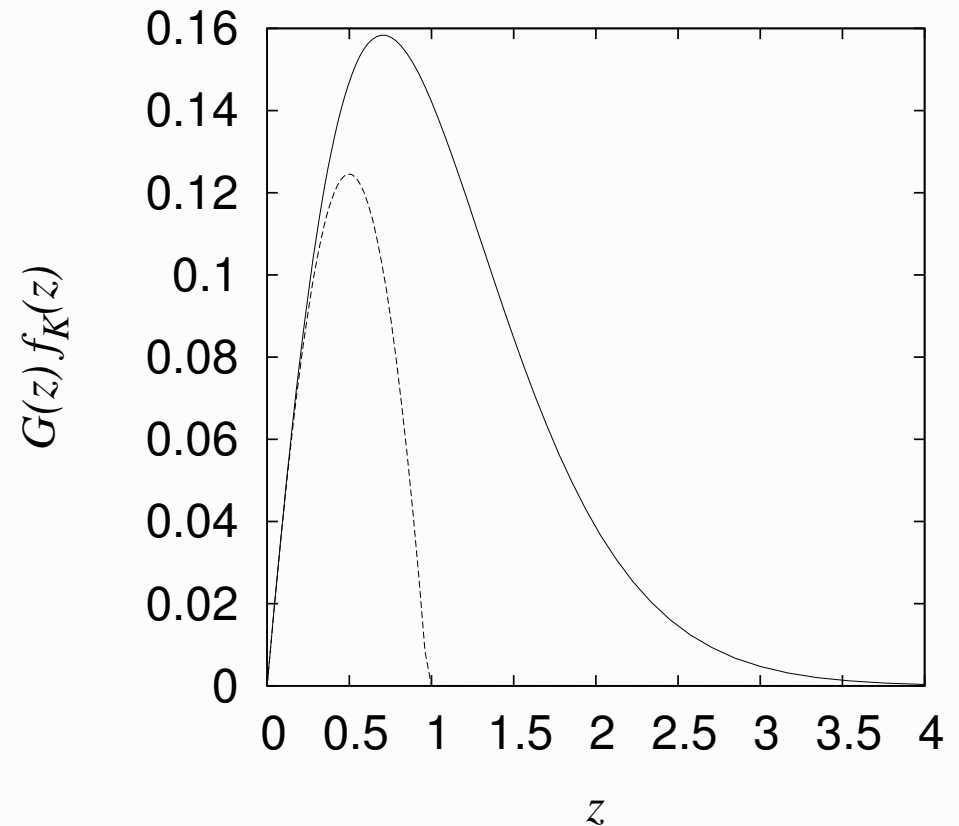
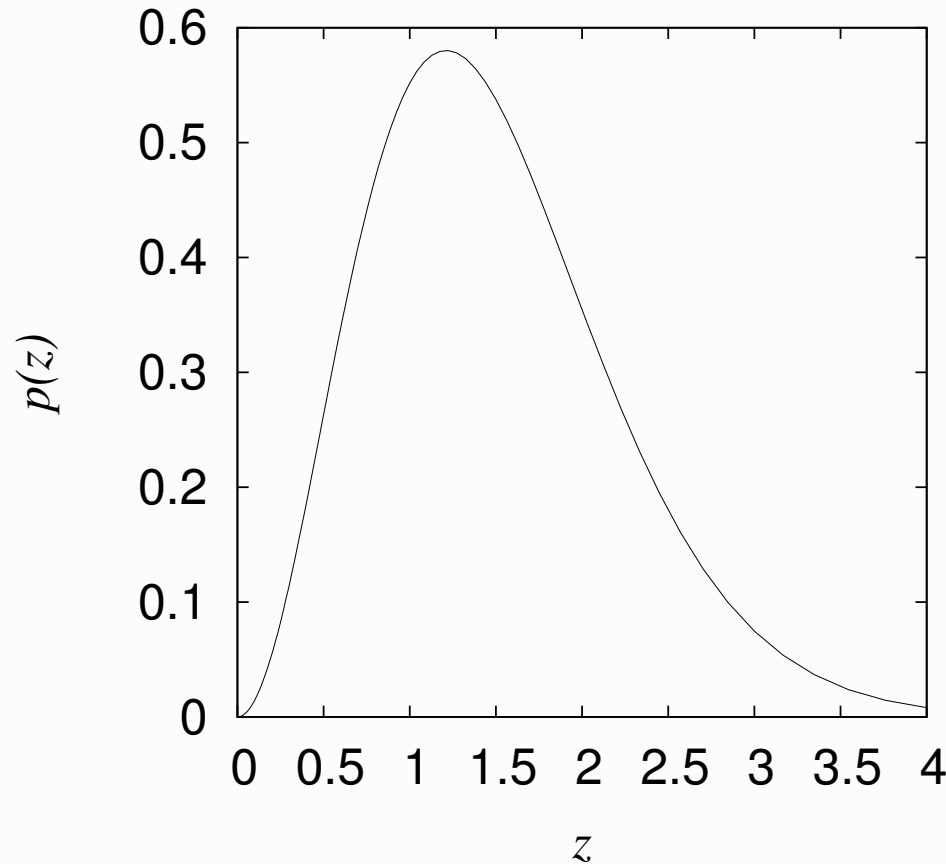
with **lens efficiency**

$$G(\chi) = \frac{3}{2} \left( \frac{H_0}{c} \right)^2 \frac{\Omega_m}{a(\chi)} \int_{\chi}^{\chi_{\text{lim}}} d\chi' p(\chi') \frac{\chi' - \chi}{\chi'}$$

The convergence is a projection of the matter-density contrast, weighted by the source galaxy distribution and angular distances.

Parametrization of redshift distribution, e.g.

$$p(z) \propto \left( \frac{z}{z_0} \right)^\alpha \exp \left[ - \left( \frac{z}{z_0} \right)^\beta \right]$$



$$\alpha = 2, \beta = 1.5, z_0 = 1$$

(dashed line: all sources at redshift 1)

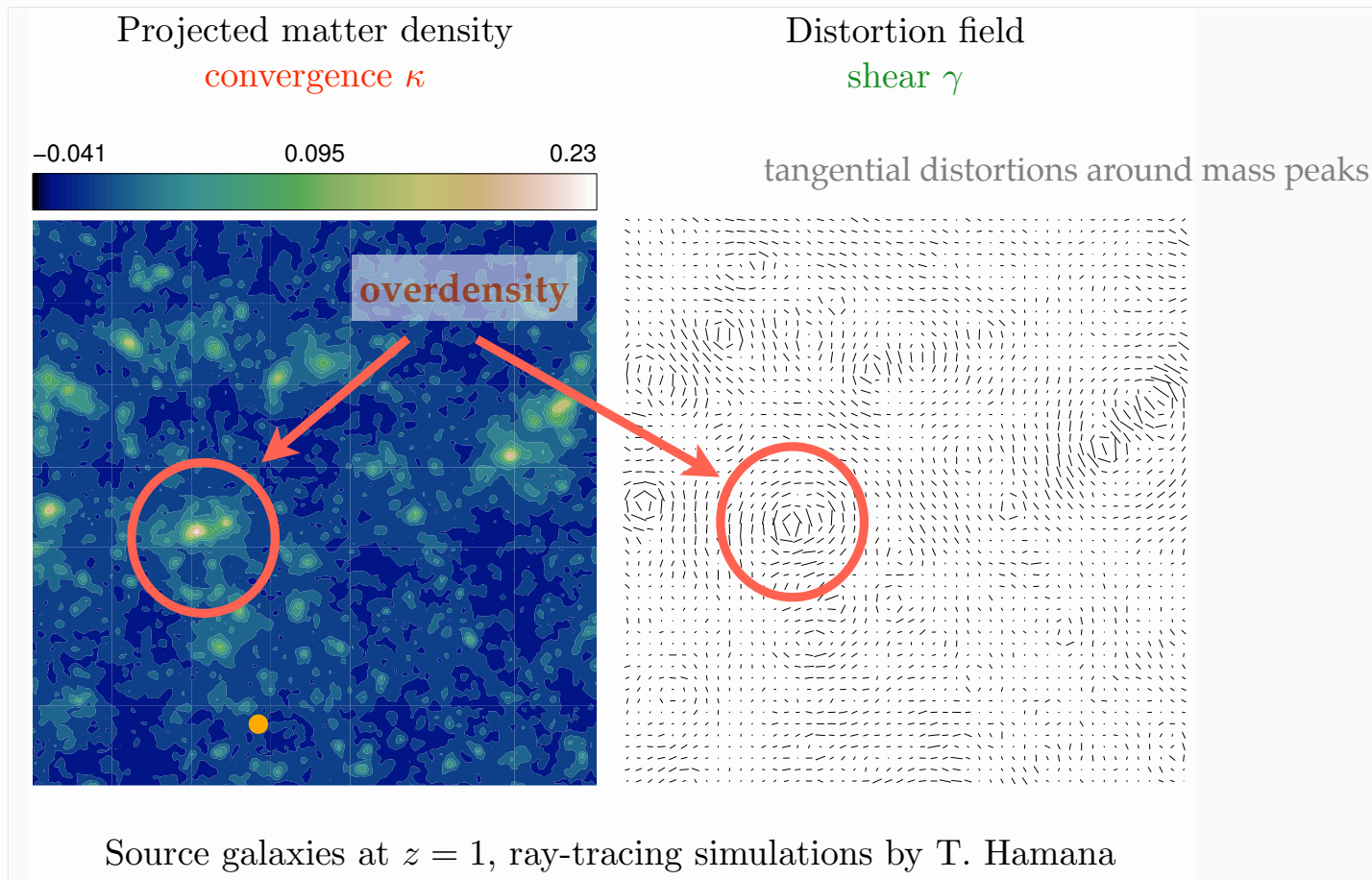
Max. lensing signal from halfway distance between us and lensing galaxies.

## More on the relation between $\kappa$ and $\gamma$

Convergence and shear are second derivatives of lensing potential  $\rightarrow$  they are related.

One can derive  $\kappa$  from  $\gamma$  (except constant *mass sheet*  $\kappa_0$ ).

E.g. get projected **mass reconstruction** of clusters from ellipticity observations.

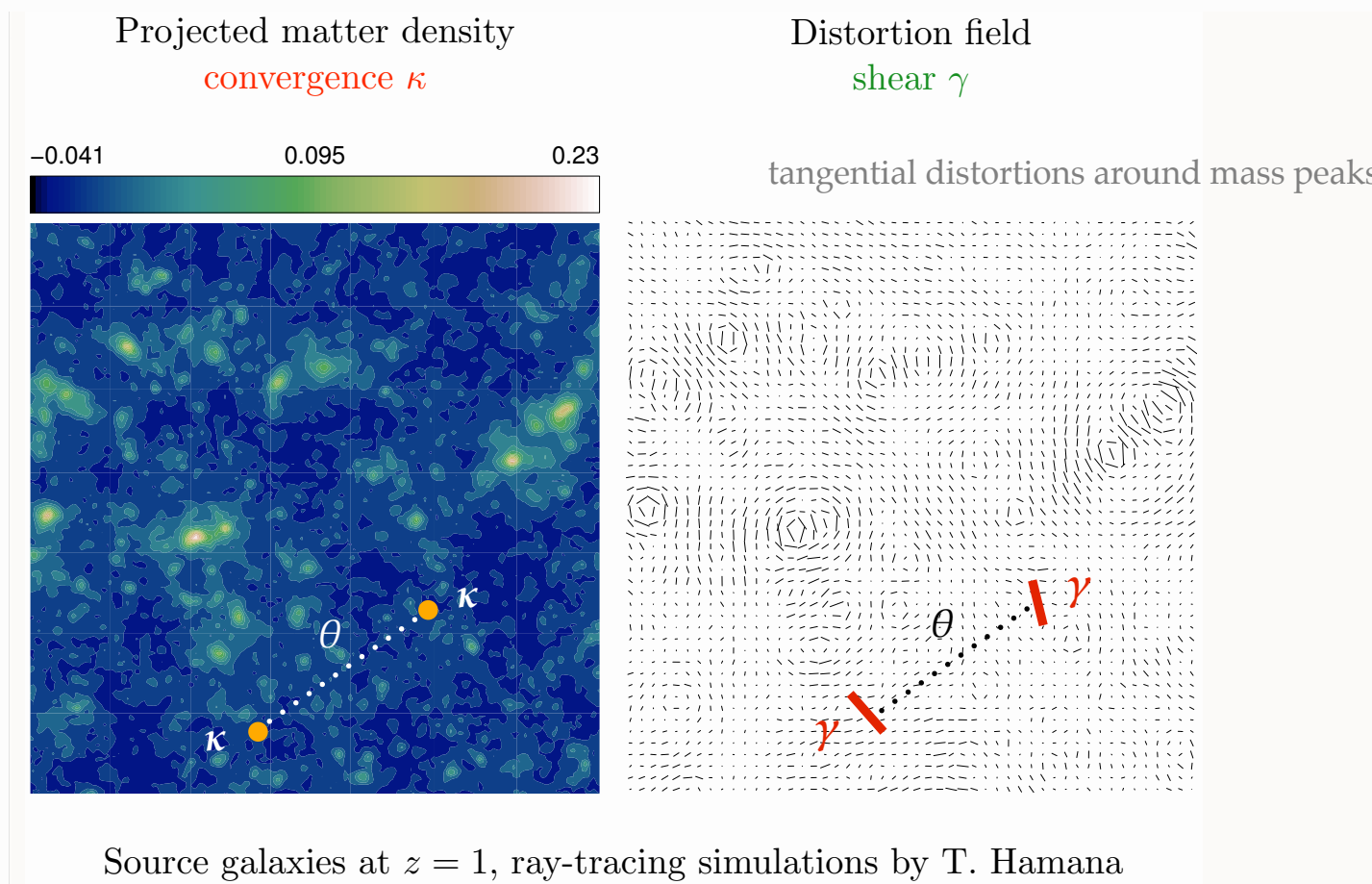


## More on the relation between $\kappa$ and $\gamma$

Convergence and shear are second derivatives of lensing potential  $\rightarrow$  they are related.

Fluctuations (variance  $\sigma^2$ ) in  $\kappa$  and  $\gamma$  are the same!

E.g. get variance/**power spectrum** of projected  $\delta$  from ellipticity correlations.



# The convergence power spectrum

- Variance of convergence  $\langle \kappa(\boldsymbol{\vartheta} + \boldsymbol{\theta})\kappa(\boldsymbol{\vartheta}) \rangle = \langle \kappa\kappa \rangle(\theta)$  depends on variance of the density contrast  $\langle \delta\delta \rangle$
- In Fourier space:

$$\langle \hat{\kappa}(\boldsymbol{\ell})\hat{\kappa}^*(\boldsymbol{\ell}') \rangle = (2\pi)^2 \delta_{\text{D}}(\boldsymbol{\ell} - \boldsymbol{\ell}') P_{\kappa}(\ell)$$

$$\langle \hat{\delta}(\mathbf{k})\hat{\delta}^*(\mathbf{k}') \rangle = (2\pi)^3 \delta_{\text{D}}(\mathbf{k} - \mathbf{k}') P_{\delta}(k)$$

- **Limber's equation**

$$P_{\kappa}(\ell) = \int d\chi G^2(\chi) P_{\delta} \left( k = \frac{\ell}{\chi} \right)$$

using small-angle approximation,  $P_{\delta}(k) \approx P_{\delta}(k_{\perp})$ , contribution only from Fourier modes  $\perp$  to line of sight. Also assumes that power spectrum varies slowly.

## Dependence on cosmology

**initial conditions,  
growth of structure**

$$P_{\kappa}(\ell) = \int d\chi G^2(\chi) P_{\delta} \left( k = \frac{\ell}{\chi} \right)$$

$$G(\chi) = \frac{3}{2} \left( \frac{H_0}{c} \right)^2 \frac{\Omega_m}{a(\chi)} \int_{\chi}^{\chi^{\text{lim}}} d\chi' p(\chi') \frac{\chi' - \chi}{\chi'}$$

**matter density**

**redshift distribution  
of source galaxies**

**geometry**



## Example

A simple toy model: single lens plane at redshift  $z_0$ ,  $P_\delta(k) \propto \sigma_8^2 k^n$ , CDM, no  $\Lambda$ , linear growth:

$$\langle \kappa^2(\theta) \rangle^{1/2} = \langle \gamma^2(\theta) \rangle^{1/2} \approx 0.01 \sigma_8 \Omega_m^{0.8} \left( \frac{\theta}{1\text{deg}} \right)^{-(n+2)/2} z_0^{0.75}$$

This simple example illustrates three important facts about measuring cosmology from weak lensing:

1. The signal is very small ( $\sim$  percent)
2. Parameters are degenerate
3. The signal depends on source galaxy redshift

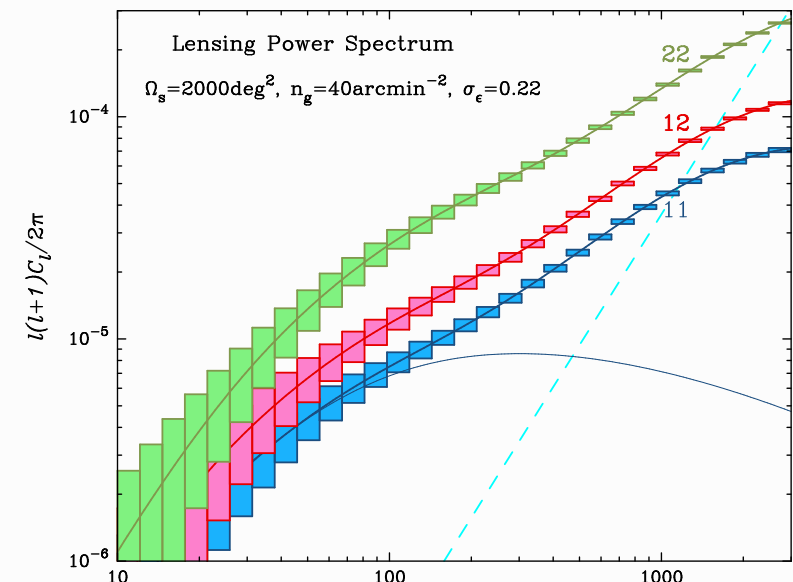
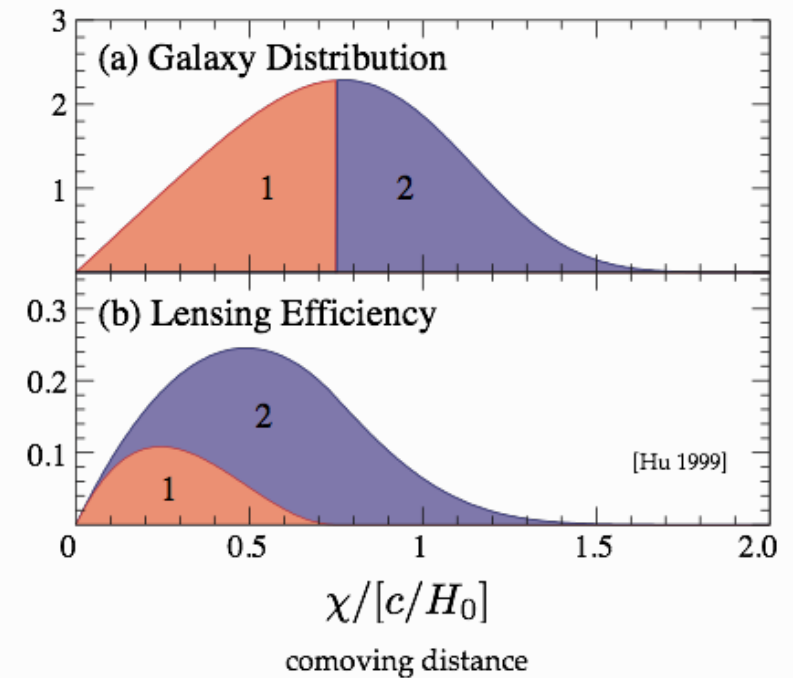
# Lensing ‘tomography’ (2 1/2 D lensing)

- Bin galaxies in redshift.
- Lensing efficiency different for different bins (even though the probed redshift range is overlapping): measure  $z$ -depending expansion and growth history.
- Necessary for dark energy, modified gravity.

$$P_{\kappa}(\ell) = \int_0^{\chi_{\text{lim}}} d\chi G^2(\chi) P_{\delta} \left( k = \frac{\ell}{\chi} \right) \rightarrow$$

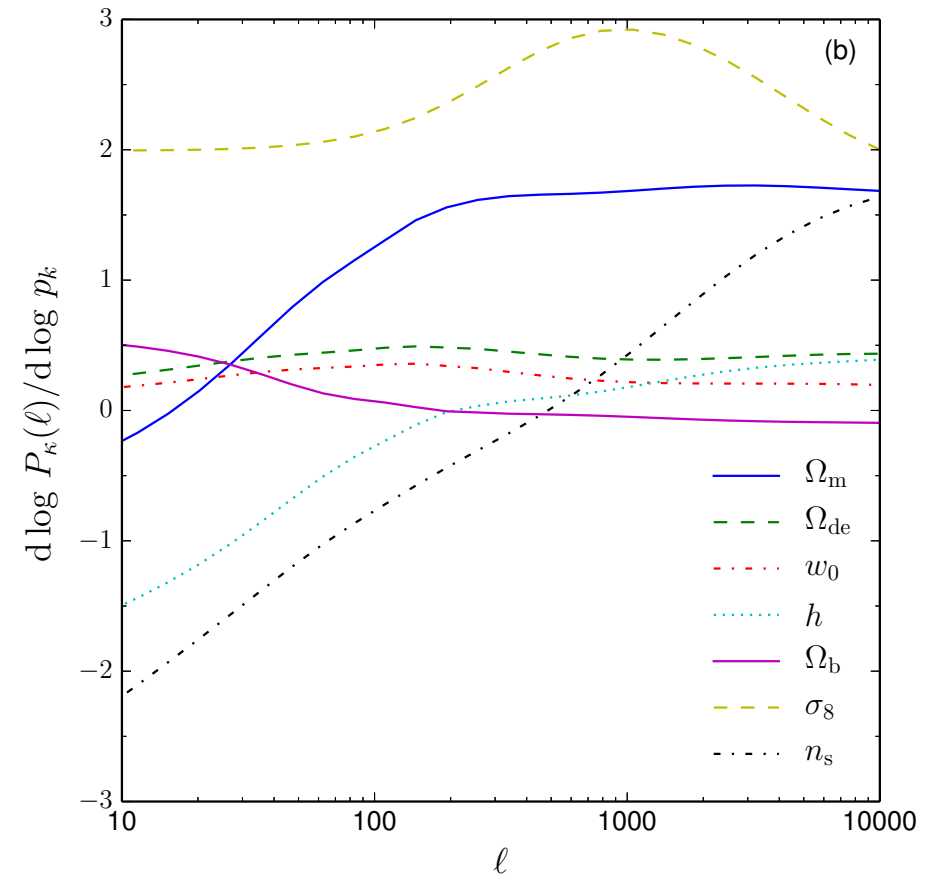
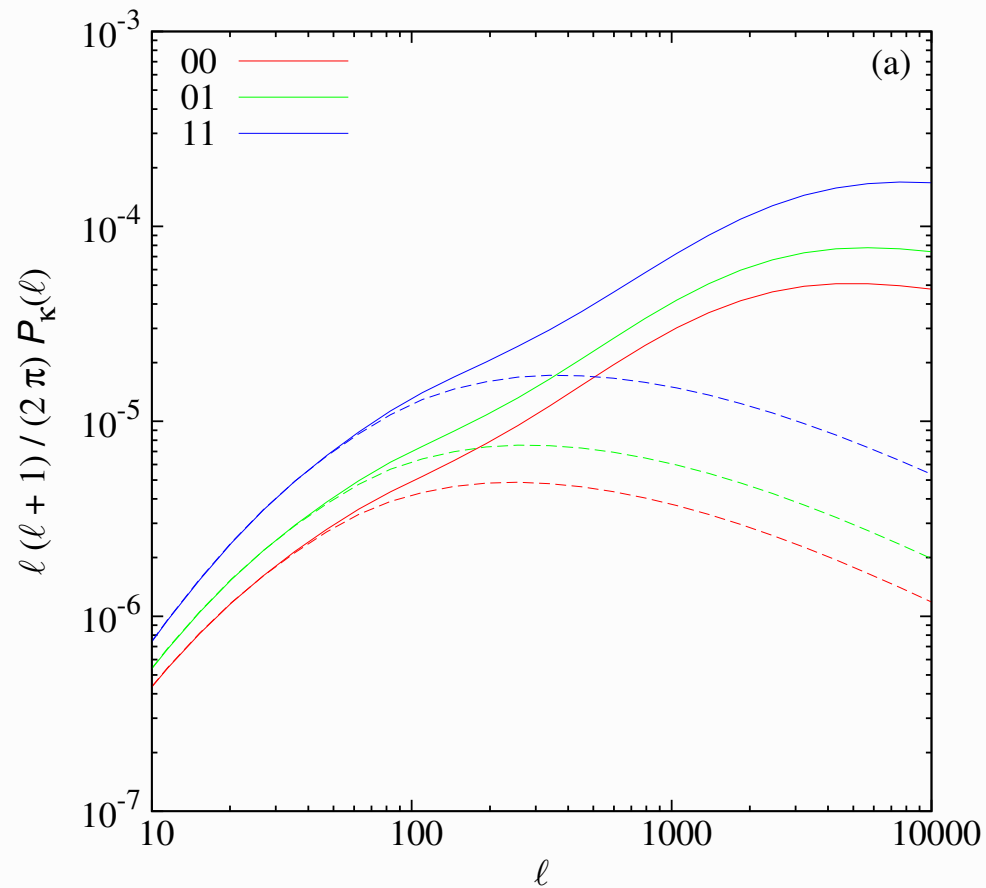
$$P_{\kappa}^{ij}(\ell) = \int_0^{\chi_{\text{lim}}} d\chi G_i(\chi) G_j(\chi) P_{\delta} \left( k = \frac{\ell}{\chi} \right)$$

$$G_i(\chi) = \frac{3}{2} \left( \frac{H_0}{c} \right)^2 \frac{\Omega_m}{a(\chi)} \int_{\chi}^{\chi_{\text{lim}}} d\chi' p_i(\chi') \frac{\chi' - \chi}{\chi'}.$$



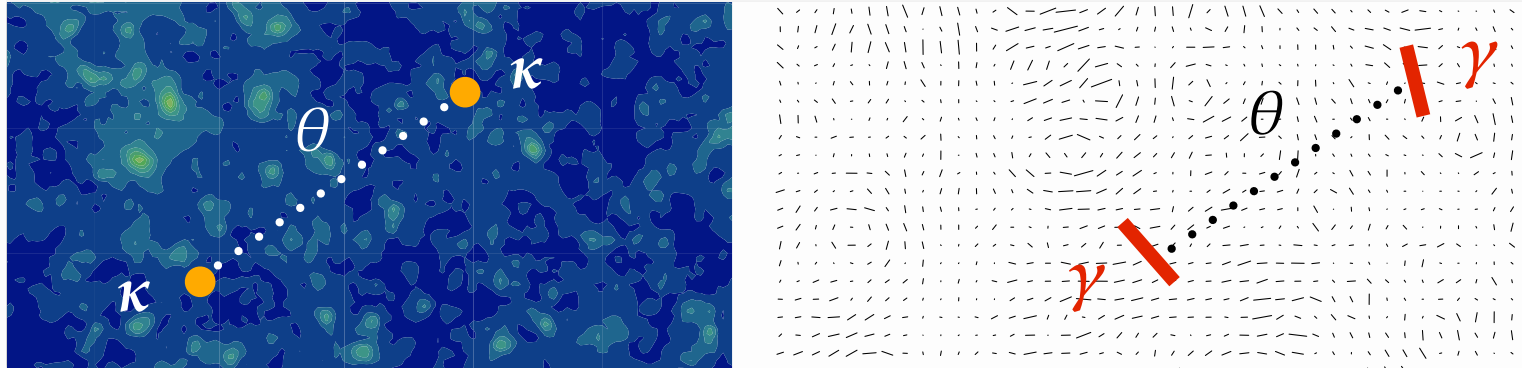
Convergence power spectrum for two different redshift bins  
( $0 = [0.5; 0.7]$ ,  $1 = [0.9; 1.1]$ ).

Unlike CMB  $C_\ell$ 's, features in matter power spectrum are washed out by projection and non-linear evolution.



## Correlations of two shears I

We have established **lensing power spectrum**  $P_\kappa = P_\gamma$  (power spectrum of projected  $\delta$ ) as interesting quantity for cosmology.



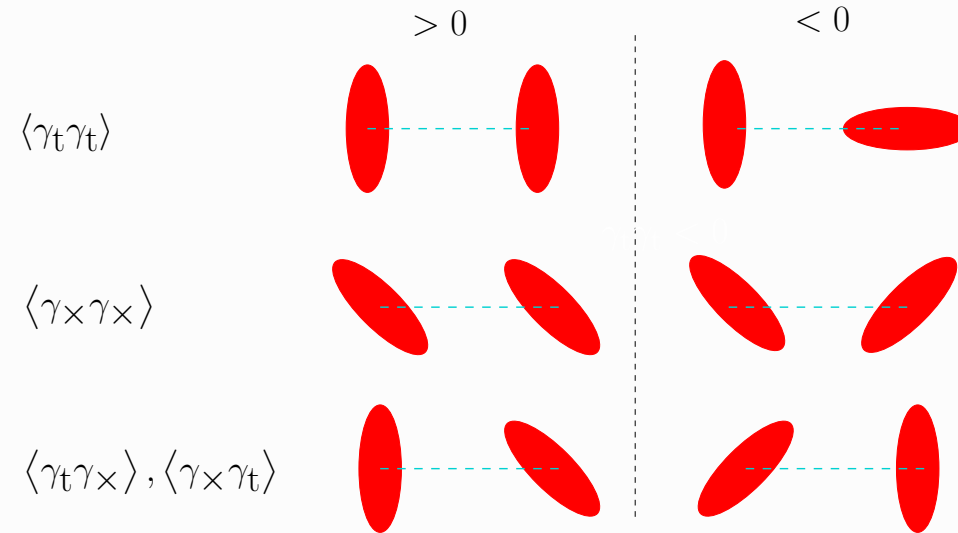
Provides theory model prediction correlation of  $\kappa$  or  $\gamma$  in Fourier space. However we measure shear (ellipticity) in real space.

Two options to make connection:

1. Fourier-transform data. Square to get power spectrum.
2. Calculate correlations in real space. Inverse-Fourier transform theory  $P_\kappa$ .

## Correlations of two shears II

Correlation of the shear at two points yields four quantities



**Parity** conservation  $\longrightarrow \langle \gamma_t \gamma_x \rangle = \langle \gamma_x \gamma_t \rangle = 0$

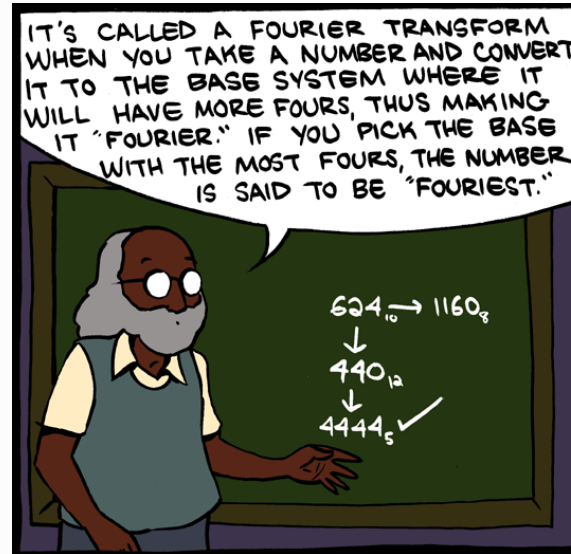
The two components of the shear **two-point correlation function** (2PCF) are defined as

$$\xi_+(\vartheta) = \langle \gamma_t \gamma_t \rangle(\vartheta) + \langle \gamma_x \gamma_x \rangle(\vartheta)$$

$$\xi_-(\vartheta) = \langle \gamma_t \gamma_t \rangle(\vartheta) - \langle \gamma_x \gamma_x \rangle(\vartheta)$$

## Correlations of two shears III

The 2PCF is the 2D Fourier transform of the lensing power spectrum.



Isotropy  $\rightarrow$  1D integrals, *Hankel transform*.

$$\xi_+(\theta) = \frac{1}{2\pi} \int_0^\infty dl \, l J_0(l\theta) P_\kappa(l)$$

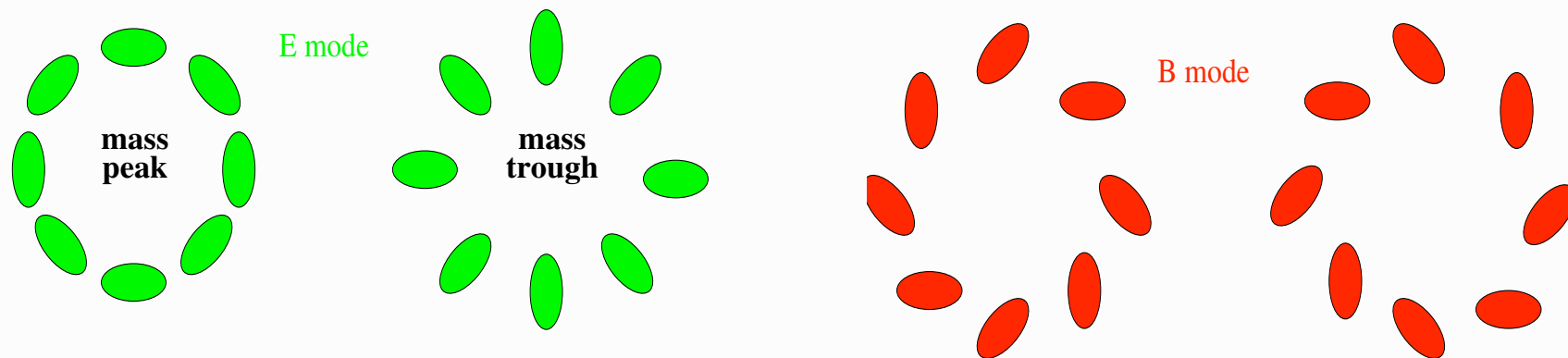
$$\xi_-(\theta) = \frac{1}{2\pi} \int_0^\infty dl \, l J_4(l\theta) P_\kappa(l),$$

# E- and B-modes I

## Shear patterns

We have seen tangential pattern in the shear field due to mass over-densities. Under-dense regions cause a similar pattern, but with opposite sign for  $\gamma$ . That results in radial pattern.

Under idealistic conditions, these are the only possible patterns for a shear field, the *E*-mode. A so-called *B*-mode is not generated.



# E- and B-modes II

## Origins of a B-mode

Measuring a non-zero B-mode in observations is usually seen as indicator of residual systematics in the data processing (e.g. PSF correction, astrometry).

Other origins of a B-mode are small, of %-level:

- Higher-order terms beyond Born approximation (propagation along perturbed light ray, non-linear lens-lens coupling), and other (e.g. some ellipticity estimators)
- Lens galaxy selection biases (size, magnitude biases), and galaxy clustering
- Intrinsic alignment (although magnitude not well-known!)
- Varying seeing and other observational effects



# E- and B-modes III

## Measuring E- and B-modes

Separating data into E- and B-mode is not trivial.

To directly obtain  $\kappa^E$  and  $\kappa^B$  from  $\gamma$ , there is leakage between modes due to the finite observed field (border and mask artefacts).

One can quantify the shear pattern, e.g. with respect to reference centre points, but the tangential shear  $\gamma_t$  is not defined at the center.

Solution: **filter** the shear map. (= convolve with a filter function  $Q$ ). This also has the advantage that the spin-2 quantity shear is transformed into a scalar.

This is equivalent to filtering  $\kappa$  with a function  $U$  that is related to  $Q$ .